



HAL
open science

Modeling of nanoparticle manipulation by AFM: Rolling vs. sliding regimes

M. Evstigneev, Karine Mougín, P. Reimann

► **To cite this version:**

M. Evstigneev, Karine Mougín, P. Reimann. Modeling of nanoparticle manipulation by AFM: Rolling vs. sliding regimes. *EPL - Europhysics Letters*, 2013, 101 (6), pp.66002. 10.1209/0295-5075/101/66002 . hal-04555422

HAL Id: hal-04555422

<https://hal.science/hal-04555422>

Submitted on 22 Apr 2024

HAL is a multi-disciplinary open access archive for the deposit and dissemination of scientific research documents, whether they are published or not. The documents may come from teaching and research institutions in France or abroad, or from public or private research centers.

L'archive ouverte pluridisciplinaire **HAL**, est destinée au dépôt et à la diffusion de documents scientifiques de niveau recherche, publiés ou non, émanant des établissements d'enseignement et de recherche français ou étrangers, des laboratoires publics ou privés.



LETTER

Modeling of nanoparticle manipulation by AFM: Rolling vs. sliding regimes

To cite this article: M. Evstigneev *et al* 2013 *EPL* **101** 66002

View the [article online](#) for updates and enhancements.

You may also like

- [Particle confinement study in hot ion H mode discharges of JT-60U](#)
H. Takenaga, K. Shimizu, N. Asakura et al.
- [Multi-Scale Mechanical-Electrochemical Modeling of Lithium-Ion Batteries](#)
Bin Wu and Wei Lu
- [Manipulation by dipole probe](#)
Takeshi Konno, Mikihiro Kobayashi,
Mitsuru Egashira et al.

Modeling of nanoparticle manipulation by AFM: Rolling vs. sliding regimes

M. EVSTIGNEEV^{1(a)}, K. MOUGIN² and P. REIMANN¹

¹ *Universität Bielefeld, Fakultät für Physik - 33615 Bielefeld, Germany, EU*

² *ICSI-CNRS - 15 Rue Jean Starcky, 68057 Mulhouse, France, EU*

received 16 January 2013; accepted in final form 5 March 2013

published online 2 April 2013

PACS 68.65.-k – Low-dimensional, mesoscopic, nanoscale and other related systems: structure and nonelectronic properties

PACS 46.55.+d – Tribology and mechanical contacts

PACS 07.79.Sp – Friction force microscopes

Abstract – We theoretically model the manipulation of a nanorod by an atomic force microscope (AFM), aiming at the determination of its sliding or rolling regimes of motion. It is found that, for contact-mode manipulation, rolling requires simultaneous fulfilment of several conditions. Namely, the corrugation of the substrate potential must be sufficiently high to overcome the effects of the particle adhesion to the substrate and to the tip. On the other hand, the corrugation of the tip potential should be relatively low to allow the particle corners to slide against the tip surface as the particle rotates. Furthermore, only sliding is possible if the tip opening angle or its radius of curvature exceed some critical values determined by the geometry of the particle cross-section.

Copyright © EPLA, 2013

What happens to a nanoparticle during manipulation by a scanning probe microscope? Why is it sometimes rolling and sometimes sliding [1–5]? These questions are of direct relevance in technological applications, where nanoparticles are used as lubricants or as building blocks in nanoelectromechanical devices. Furthermore, they are of basic importance for our understanding of the laws of nature acting at the nanoscale. Perhaps, the main difficulty to answer these questions theoretically is an extended hierarchy of relevant time scales, covering about nine orders of magnitude. The fastest one characterizes the vibration period of single atoms (subpicosecond range). Next, the center of mass of the nanoparticle exhibits oscillations in the potential of the substrate on the nanosecond scale. The oscillation period of the tip is in the microsecond region. Finally, the slowest time scale derives from the translational motion of the probe, which typically covers only a few lattice constants in a millisecond.

Accordingly, theoretical models of nanomanipulation can be divided into two main groups: atomistic [6–8] and continuous [9,10] ones. Atomistic modeling gives insight into the fine details of the manipulation process. At the same time, the large separation of time scales imposes severe limitations on the direct atomistic simulation of

the problem, both with respect to the number of atoms (typically, a few thousand) and pulling velocities (typically, meters per second) [7].

Continuous models [9,10] usually treat a nanoparticle as a regularly shaped object (*e.g.*, a sphere) described by the “macroscopic” concepts of contact mechanics. In contrast to atomistic models, continuous models are applicable to relatively large particles, where some important mechanisms related to their specific molecular structure are unimportant. However, such a description becomes inappropriate for nanoparticles for several reasons [11,12]. Among others, due to the unavoidable deviations from perfect rotational symmetry, the surface of a nanoparticle actually consists of facets [1–5]. In particular, regularly faceted nanorods can be synthesized with a remarkably large variety of polygonal shapes: triangular [13], square [14], pentagonal [15], hexagonal [16], octagonal [17], etc. Then, the contact properties of a nanoparticle with a flat substrate—such as its friction coefficient—should depend on the particle’s orientation and may be very different if the contact is formed along the nanoparticle facet or along one of the edges separating two adjacent facets.

We present a coarse-grained hybrid model combining the strengths of the two approaches: atomistic and continuous. On the one hand, it is fast enough to be

^(a)E-mail: mykhaylo@physik.uni-bielefeld.de

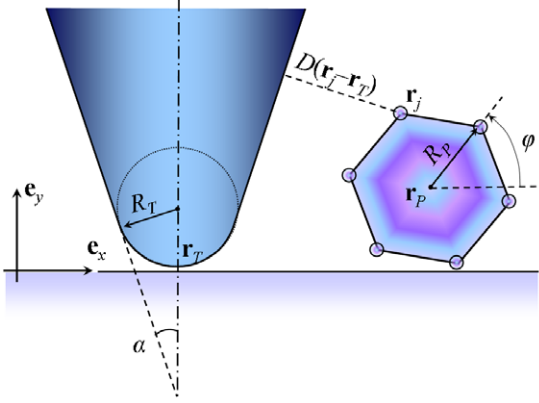


Fig. 1: (Colour on-line) The model: an N -sided nanoparticle of radius R_P is pushed by a conical AFM tip (opening angle α) smoothly joined to a spherical apex of radius R_T . The particle configuration is specified by its center of mass \mathbf{r}_P and rotation angle φ , and the tip configuration by the apex position \mathbf{r}_T .

computationally feasible on a laptop; on the other hand, it is sufficiently detailed to make predictions about geometry- and interaction-dependent regimes of sliding and rolling motion of the nanoparticle. Specifically, the model is applied to describe the contact-mode manipulation of a regularly shaped nanorod on a periodic substrate by a conical AFM tip with a rounded apex.

To exclude the possibility of in-plane rotation of the nanorod around an axis perpendicular to the substrate, we assume that it is pushed in the middle and focus on a two-dimensional description, as indicated in fig. 1. Due to the large time scale separation, it is safe to assume that atomic degrees of freedom are, at each moment of time, in thermodynamic equilibrium constrained by the given values of the nanoparticle's center of mass position, \mathbf{r}_P , its rotation angle, φ , and the tip apex position, \mathbf{r}_T , see fig. 1. A further assumption is that all deformations are elastic and occur on a time scale much faster than that of the translational and rotational motion of the nanoparticle. Finally, we focus on the case where the tip adhesion to the substrate is sufficiently strong and the cantilever is sufficiently rigid, so that the tip hardly moves vertically or torsionally during manipulation. Thus, the tip apex position \mathbf{r}_T is a time-dependent vector,

$$\mathbf{r}_T(t) = \mathbf{e}_x(x_T(0) + Vt), \quad (1)$$

describing a contact-mode motion with constant velocity V in x -direction and zero y -component.

The large time scale separation between the slow cantilever tip and the fast particle coordinates allows us to introduce the potential energy (more precisely, the free energy), $U(\mathbf{r}_P, \varphi; \mathbf{r}_T)$, which is a unique function of the coordinates \mathbf{r}_P and φ at a given tip position \mathbf{r}_T . It also allows us to assume that the particle always finds itself in the mechanical equilibrium corresponding to the

instantaneous position of the tip:

$$\frac{\partial U(\mathbf{r}_P(t), \varphi(t); \mathbf{r}_T(t))}{\partial(\mathbf{r}_P, \varphi)} = 0 \quad (2)$$

for a rather wide range of experimentally relevant velocities V . The thermal fluctuations of the fast atomic degrees of freedom are thus accounted for by the free energy-type potential $U(\mathbf{r}_P, \varphi; \mathbf{r}_T)$, while the much weaker remnant thermal fluctuations of the much slower collective degrees of freedom \mathbf{r}_P and φ are considered negligible in eq. (2).

As a convenient means of parameterizing the potential energy, we employ the concept of pseudoatoms, representing the collective effect of large atomic groups. For an N -sided nanoparticle from fig. 1, the simplest choice consists in N pseudoatoms located in the nanoparticle's corners. The position \mathbf{r}_j of the j -th pseudoatom is then determined by the coordinates \mathbf{r}_P and φ as

$$\mathbf{r}_j(\mathbf{r}_P, \varphi) = \mathbf{r}_P + R_P [e_x \cos(\varphi + 2\pi j/N) + e_y \sin(\varphi + 2\pi j/N)]. \quad (3)$$

The potential energy is written as a sum over all pseudoatoms,

$$U(\mathbf{r}_P, \varphi; \mathbf{r}_T) = \sum_j [u_S(\mathbf{r}_j) + u_T(\mathbf{r}_j - \mathbf{r}_T)], \quad (4)$$

where the two terms in the sum are the interaction energies of the j -th pseudoatom with the substrate and the tip. By a suitable choice of the individual pseudoatom potentials and, if necessary, by changing the number of pseudoatoms and adjusting their relative location, it is possible to reproduce any realistic potential $U(\mathbf{r}_P, \varphi; \mathbf{r}_T)$. At the same time, it is clear that the main parameters that determine sliding or rolling of the nanoparticle are adhesion and corrugation of the substrate and tip potentials. Therefore, we focus for simplicity on the following first-order Fourier expansion for the former:

$$u_S(\mathbf{r}) = \frac{\varepsilon_S}{\beta - 1} \left[\left(\frac{\sigma}{y} \right)^\beta - \frac{\beta\sigma}{y} \right] + \Delta U \left(\frac{\sigma}{y} \right)^\beta \cos \frac{2\pi x}{a}. \quad (5)$$

The first term describes the effect of adhesion with adhesion energy ε_S , equilibrium separation σ , and exponent $\beta > 1$. Its attractive part is chosen to decay inversely proportional to y , reflecting the van der Waals interaction between two extended objects, which are separated by distances much smaller than their own linear dimensions [18]. Its repulsive part results from the steric interaction and elastic deformation of the two objects in close contact. The second term in (5) accounts for the substrate corrugation in x -direction. Since it is rooted in the same type of short-range interaction as the steric and elastic repulsion, we have chosen the same $y^{-\beta}$ -dependence of both terms. Physically, we should have $|\Delta U| < \varepsilon_S/(\beta - 1)$, so that the corrugation term, which can be both positive and negative, never overrules the repulsive first term at small separations y .

Our main objective is to find the conditions necessary for rolling. Therefore, we should focus on the most “rolling-friendly” case from the very beginning. We have verified numerically that tip corrugation and adhesion only hinder rolling: at finite adhesion, the particle sticks to the tip with one of its facets, while corrugation prevents the particle corners from sliding against the tip surface as the particle is rolling. Therefore we exclude these effects from our consideration. In reality, adhesion forces between the nanorod and the tip cannot be turned off; however, they can be made small in comparison to the particle-substrate adhesion by increasing the nanoparticle length. The reason is that, for a long nanorod, its contact area with the substrate, and hence the corresponding interaction energy, both scale linearly with length, whereas the particle-tip contact area is length independent. Denoting the distance from the tip surface to the j -th pseudoatom by $D(\mathbf{r}_j - \mathbf{r}_T)$, see fig. 1, we assume that the particle-tip interaction potential is thus of purely repulsive form:

$$u_T(\mathbf{r}_j - \mathbf{r}_T) = \varepsilon_T \left(\frac{\sigma}{D(\mathbf{r}_j - \mathbf{r}_T)} \right)^\beta. \quad (6)$$

Next, we specify the model parameters in eqs. (5), (6) and fig. 1. We set the substrate adhesion energy, ε_S , and its lattice constant, a , to one, thus fixing our units of energy and length. The equilibrium separation σ in (5) is typically comparable to the lattice constant a , hence, we choose $\sigma = 1$. With respect to the short-range repulsion in (5) and (6), there remains a certain arbitrariness in the choice of the exponent β and the prefactor ε_T in eqs. (5) and (6). Fortunately, the character of motion of the nanoparticle (rolling or sliding) turns out to be practically independent of this choice, as we have verified by extensive numerical simulations. Below, we present the results obtained for $\beta = 4$ and $\varepsilon_T = 1$. Turning to fig. 1, the radius of the nanorod R_P is chosen so that its facet length is equal to thirty lattice constants. The tip radius R_T is chosen to be smaller than the particle radius, *i.e.* the particle is manipulated by the flat part of the tip.

In order to solve (1)–(6) with the above-specified parameters numerically, time is discretized into small steps. At each step, the tip (1) is first moved by a tiny fraction of the lattice constant of the substrate. Then, the local minimum is determined with respect to the “fast coordinates” \mathbf{r}_P and φ at the fixed new \mathbf{r}_T according to eq. (2). In particular, this new local minimum must belong to the same basin of attraction as the current values of \mathbf{r}_P and φ .

Figure 2 shows which manipulation regime of a hexagonal nanoparticle is realized depending on the substrate corrugation ΔU and tip opening angle α . For $\alpha < \pi/3$, rolling is realized for ΔU exceeding some α -dependent threshold, which turns out to be particularly high for tip opening angles close to $\pi/6$ and $\pi/3$. The behavior beyond the realm shown in fig. 2 is as suggested by fig. 2 itself: For $\alpha > \pi/3$, only sliding is observed, and beyond $\Delta U = 0.22$,

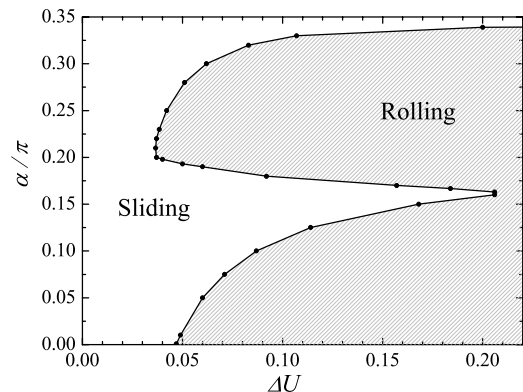


Fig. 2: State diagram showing which regime of motion of a hexagonal nanoparticle ($N = 6$) is realized depending on the corrugation of the substrate potential ΔU and the tip opening angle α .

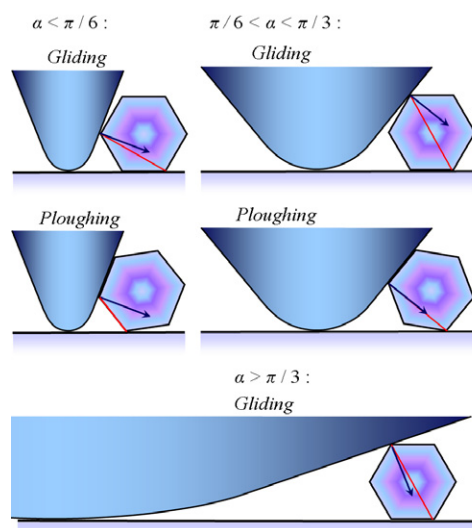


Fig. 3: (Colour on-line) Gliding and ploughing configurations of a hexagonal nanoparticle in the sliding manipulation mode. Blue arrows and red lines are explained in the main text.

the almost horizontal border at $\alpha \simeq \pi/3$ between rolling and sliding regimes continues up to the maximum ΔU -value of $\varepsilon_S/(\beta - 1) = 1/3$ (see above).

To better understand these findings, we first observe that those configurations, where both contacts of the nanoparticle with the substrate and the tip are formed by its corners, are unstable: any small rotation of the nanoparticle from such a configuration will lead to the onset of a torque favoring further rotation in the same direction. Therefore, sliding of a nanoparticle necessarily requires that its contact either with the substrate or with the tip is formed by one of its facets. The respective configurations will be henceforth denoted as *gliding* and *ploughing* modes, see fig. 3. If both gliding and ploughing configurations are unstable, the particle will be rolling.

To maintain rolling, one pseudoatom in contact with the substrate must always serve as a pivoting point, similar to the mechanism described in ref. [3]. This is only possible if the substrate corrugation is sufficiently high to overcome its adhesion. In agreement with fig. 2, a first indispensable prerequisite for rolling is thus a not too small value of ΔU . Since the N model pseudoatoms encapsulate the collective effect of large groups of real atoms, the corrugation parameter ΔU effectively takes into account also the atomistic commensurability of substrate and particle facets. Thus, our above condition on ΔU correlates well with the experimental findings of Falvo *et al.*, who report sliding of carbon nanotubes on mica surface and rolling on graphite, hence suggesting that “commensurate contact is a necessary condition for rolling” [1].

Besides this energy condition, there is a second, geometric requirement that needs to be fulfilled in order for the nanoparticle to roll: namely, a small rotation of the nanoparticle out of the gliding or ploughing configuration in the negative (clockwise) direction must result in a torque produced by the tip in the same direction. The sign of this torque can be readily determined for the particle-tip interaction potential (6), where the force produced by the tip on the particle is perpendicular to the tip surface. Namely, if the tip normal (fig. 3, blue arrows) at the point of tip-particle contact lies above the line joining this contact point with the pivot point (fig. 3, red lines), then the torque is negative and favors rolling; otherwise, it is positive and promotes sliding.

Applying this criterion to a hexagonal particle, we can conclude that sliding is the only contact-mode manipulation regime possible for a rigid tip with opening angle $\alpha > \pi/3$, see fig. 3, as indeed found numerically in fig. 2. If $\alpha < \pi/6$, then the torque produced by the tip is negative for both gliding and ploughing configuration, so that the particle can roll, provided that the substrate corrugation ΔU is sufficiently high. If α is between $\pi/6$ and $\pi/3$, then the torque produced by the tip is negative in the gliding configuration and vanishes in the ploughing state. But a small rotation out of the ploughing configuration in the clockwise direction induces a small torque in the same direction, and therefore rolling out of the ploughing state is not excluded. Finally, if the tip opening angle is close to the value $\pi/6$, then the particle’s contacts both with the tip and the substrate are formed by its facets. In this case, rolling is difficult, because of the adhesion of the particle to the substrate and due to the fact that the torque induced by a small rotation of the particle is small.

Likewise, by applying similar reasoning to nanoparticles of different cross-sections, we now can predict their sliding or rolling depending on the geometry of the tip. In particular, we predict that a triangular nanorod ($N = 3$) can never roll during contact-mode manipulation by a rigid tip. In the case $N = 4$ (square cross-section), only sliding will be realized for tip opening angles $\alpha > \pi/4$, with the possibility of rolling for $\alpha < \pi/4$ and sufficiently large ΔU . Rolling of a pentagonal nanoparticle ($N = 5$)

is possible for $\alpha < \pi/5$. In the range $\pi/5 < \alpha < 3\pi/10$, the particle will be gliding, and for $3\pi/10 < \alpha < 2\pi/5$, the gliding configuration becomes unstable, if ΔU is sufficiently large. Then, the particle will turn into a ploughing configuration, with further rolling being hindered by geometric constraints. Finally, for $\alpha > 2\pi/5$, the gliding configuration becomes stable again. The shape of the state diagram for an octagonal particle ($N = 8$) is similar to fig. 2. Namely, for $\alpha > 3\pi/8$, the only manipulation regime possible is sliding. For $\alpha < \pi/4$ and $\pi/4 < \alpha < 3\pi/8$, the particle can roll, provided that ΔU is sufficiently large. Near $\alpha \simeq \pi/4$, the nanoparticle forms contacts with both tip and substrate via its facets, with sliding being the preferred regime of motion.

Although we have limited ourselves to tip radii R_T smaller than the particle radius R_P , these considerations can be immediately extended to $R_T > R_P$. In this case, the tip surface can still be regarded as practically flat on the length scales comparable to the length of the facet in contact with the tip. By approximating the particle cross-section with a circle centered at \mathbf{r}_P , we find that the angle α^* formed by the tip normal at the point of contact and the substrate is related to the tip radius as

$$R_T = R_P \frac{1 + \sin \alpha^*}{1 - \sin \alpha^*}. \quad (7)$$

Manipulation by a tip with $R_T > R_P$ will have a similar outcome as manipulation by a tip with $R_T < R_P$ and a “renormalized” opening angle α^* given by (7). Substitution into eq. (7) of the highest tip opening angle α^{max} for which rolling is still possible in the case $R_T < R_P$ gives the largest tip radius R_T^{max} , such that the particle will only slide if $R_T > R_T^{max}$. In particular, for a square particle we find $\alpha^{max} = \pi/4$, and hence it can only slide if $R_T > R_T^{max} \simeq 6R_P$; sliding of a pentagonal particle ($\alpha^{max} = \pi/5$) is guaranteed for $R_T > 4R_P$; a hexagonal particle ($\alpha^{max} = \pi/3$) will slide for $R_T > 14R_P$; an octagonal particle ($\alpha^{max} = 3\pi/8$) slides for $R_T > 25R_P$.

In conclusion, we have introduced a model that allows one to study manipulation of a nanorod by an AFM. We have applied our model to the contact-mode manipulation by a rigid AFM cantilever and found that, in contrast to our everyday “macroscopic” experience, rolling of a nanoparticle is a special regime of motion, which requires simultaneous fulfilment of several conditions. Namely, the corrugation of the substrate potential must be high enough to overcome the effects of particle adhesion to the substrate and to the tip. Furthermore, rolling is only possible if the tip opening angle and/or the tip radius is smaller than some value determined by the geometry of the nanoparticle cross-section; otherwise, sliding is the only possible manipulation mode. The model can be easily modified to include the effects that we have left out in the present paper, such as finite rigidity of the tip, its adhesion and corrugation, and its oscillations in the tapping manipulation mode.

We are grateful to the Deutsche Forschungsgemeinschaft (Collaborative Research Center SFB 613 and RE 1344/6) and the ESF programs NATRIBO and FANAS (collaborative research project Nanoparma) for financial support.

REFERENCES

- [1] FALVO M. R., TAYLOR R. M. II, HELSER A., CHI V., BROOKS F. P. jr, WASHBURN S. and SUPERFINE R., *Nature*, **397** (1999) 236; FALVO M. R., STEELE J., TAYLOR R. M. II and SUPERFINE R., *Tribol. Lett.*, **9** (2000) 73.
- [2] RITTER C., HEYDE M., SCHWARZ U. D. and RADEMANN K., *Langmuir*, **18** (2002) 7798.
- [3] KEELING D. L., HUMPHRY M. J., FAWCETT R. H. J., BETON P. H., HOBBS C. and KANTOROVICH L., *Phys. Rev. Lett.*, **94** (2005) 146104.
- [4] GRILL L., RIEDER K.-H., MORESCO F., RAPENNE G., STOJKOVIC S., BOJU X. and JOACHIM C., *Nat. Nanotechnol.*, **2** (2007) 95.
- [5] TEVET O., VON-HUTH P., POPOVITZ-BIRO R., ROSENSTVEIG R., WAGNER H. D. and TENNE R., *Proc. Natl. Acad. Sci. U.S.A.*, **108** (2011) 19901.
- [6] MARTSINOVICH N. and KANTOROVICH L., *Nanotechnology*, **20** (2009) 135706.
- [7] MAHBOOBI S. H., MEGHDARI A., JALILI N. and AMIRI F., *Physica E*, **42** (2009) 182.
- [8] BULDUM F. and LU J. P., *Phys. Rev. Lett.*, **83** (1999) 5050.
- [9] SITTI M., *IEEE/ASME Trans. Mechatron.*, **8** (2009) 1.
- [10] KORAYEM M. H. and ZAKERI M., *Int. J. Adv. Manuf. Technol.*, **41** (2009) 714.
- [11] MO Y., TURNER K. T. and SZLUFARSKA I., *Nature*, **457** (2009) 1116.
- [12] LUAN B. and ROBBINS M. O., *Nature*, **435** (2005) 929.
- [13] MILLSTONE J. E., HURST S. J., MÉTRAUX G. S., CUTLER J. I. and MIRKIN C. A., *Small*, **5** (2009) 646.
- [14] SAU T. and MURPHY C. J., *J. Am. Chem. Soc.*, **126** (2004) 8648; JIN R., EGUSA S. and SCHERER N. F., *J. Am. Chem. Soc.*, **126** (2004) 9900.
- [15] DOROGIN L. M., VLASSOV S., KOLESNIKOVA A. L., KINK I., LÖHMUS R. and ROMANOV A. E., *J. Nanosci. Nanotechnol.*, **10** (2010) 6136.
- [16] TRANVOUEZ E., ORIEUX A., BOER-DUCHEMIN E., DEVILLERS C. H., HUC V., COMTET G. and DUJARDIN G., *Nanotechnology*, **20** (2009) 165304.
- [17] WANG Z. L., MOHAMED M. B., LINK S. and EL-SAYED M. A., *Surf. Sci.*, **440** (1999) L809.
- [18] ISRAELACHVILI J. N., *Intermolecular and Surface Forces* (Academic Press, London) 1992.